



TITLE:

# Instability of electron cyclotron harmonics in a beam-plasma system( Dissertation\_全文 )

AUTHOR(S):

Idehara, Toshitaka

---

CITATION:

Idehara, Toshitaka. Instability of electron cyclotron harmonics in a beam-plasma system.  
京都大学, 1968, 理学博士

ISSUE DATE:

1968-03-23

URL:

<https://doi.org/10.14989/doctor.k755>

RIGHT:



---

學位申請論文

---

---

出原敏孝

---



Instability near Electron Cyclotron Harmonics in

Beam-Plasma System\*

(電子ビームとプラズマとからなる系における電子サイクロ  
トロン高調波の不安定性)

Toshitaka IDEHARA

Department of Physics, Faculty of Science,

University of Kyoto, Kyoto

(Received Oct. 31, 1967)

# Synopsis

Instabilities near harmonics of the electron cyclotron frequency are observed when a weak electron beam is injected into a plasma in nearly thermal equilibrium. Measurements of microwave emission show that the electron cyclotron harmonics are enhanced strongly by the electron beam passing through the plasma, and that at the same time the second harmonics of the enhanced cyclotron harmonics are generated by a nonlinear effect in plasmas. The experimental results are interpreted by means of the model of a Maxwellian plasma penetrated by a monoenergetic electron beam.

---

\* Reported in part in J. Phys. Soc. Japan 23 (1967) 660.

## §1 Introduction

In the last few years, considerable interests have been built up in the problem of electron cyclotron harmonics in plasma. Landauer<sup>1)</sup> could find the electron cyclotron harmonic emissions up to the 45th, by observing noise emission from the PIG discharge. For explaining the result, Canobbio and Croci<sup>2)</sup> ascribed the harmonic emissions to the electrostatic waves which are excited by superthermal electrons existing in PIG discharge and propagate perpendicular to the magnetic field. On the other hand, Mitani, Kubo and Tanaka<sup>3)</sup> observed the cyclotron harmonic emissions in the low pressure arc discharge as well. Examining the dispersion characteristics of these emissions, they showed that they correspond to the longitudinal plasma oscillations in the magnetic field, which are suggested by Bernstein.<sup>4)</sup> Many authors<sup>5)</sup> discussed these electrostatic waves near cyclotron harmonics in a collisionless plasma, and showed that they can propagate perpendicular to the magnetic field without Landau damping.

In the case of the propagation parallel to the static magnetic field or more generally, in the case of the propagation oblique to the magnetic field, the Landau damping plays an important role and therefore, the cyclotron harmonic waves damp out and can not propagate in a Maxwellian plasma. However, in a plasma with an electron beam running along the magnetic field, the growing cyclotron harmonic waves propagating parallel to the magnetic field are expected, because the electron beam excites the wave strongly to overcome Landau damping. Gruber et al.<sup>6)</sup> and Bekefi et al.<sup>7)</sup> observed the cyclotron harmonic wave growing along the magnetic field in a beam-generated plasma.

This result may be explained by a convective instability produced by the coupling of cyclotron harmonic waves in a plasma with a slow space charge wave in a beam, in the case of the oblique propagation.

The micro-instability of the electron cyclotron harmonics have been investigated in detail by Harris.<sup>8)</sup> This instability, which is an absolute one, results from the anisotropy of the electron distribution in velocity space. From the point of view of the beam-plasma interaction, Crawford et al.<sup>9)</sup> proposed that this instability is produced by an interaction of the cyclotron harmonic waves in plasma with the cyclotron harmonic waves having negative energies in the beam. This phenomenon is also expected to occur in the beam-plasma system.

In order to study this instability experimentally, we inject an electron beam into a nearly Maxwellian plasma which is produced independently of the beam, and therefore, we can change parameters of the plasma and the beam independently. Thus, comparing our present results with those reported up to the present where either an electron beam is considered to be present in the plasma spontaneously or the plasma is produced by injecting the electron beam into the neutral gas, we can obtain more detailed informations on this instability.

The contents of the following paragraphs are as follows: The microwave emission are measured when the electron beam is injected into the nearly Maxwellian plasma. From the experimental results the electron cyclotron harmonic waves propagating nearly perpendicular to the magnetic field are considered to be strongly enhanced by the above mentioned absolute instability. When the cyclotron

harmonic emissions are enhanced strongly, their second harmonics are generated by a nonlinear effect. Experimental results are analyzed by the theory of Crawford et al.<sup>9)</sup>

## §2 Experimental apparatus and procedures

In order to investigate the instabilities of plasma due to the presence of an electron beam, it is desired that a highly ionized and Maxwellian plasma is produced and an electron beam is injected into this plasma. To obtain such a beam-plasma system, we have set up the apparatus which is consisted of three regions, that is, the dc discharge region, the plasma-diffused region and the beam-produced region, as shown in Fig. 1. Argon gas of the pressure of about  $10^{-1}$  torr is fed into the discharge region and, by using a method of differential pumping, the gas pressures of the plasma-diffused and the beam-produced regions are maintained at about  $5 \times 10^{-4}$  and  $7 \times 10^{-6}$  torr respectively. An external magnetic field is applied along the tube axis and its intensity distribution on the axis is shown in Fig. 1. In the discharge region the plasma is produced by a dc discharge between a cathode situated at the center of the cusped geometry and an anode situated near the point cusp. The discharge current  $I_d$  is varied from 2mA to 4.5A. This plasma is diffused through a hole (8 mm in diameter) at the center of the anode into the plasma-diffused region along the external magnetic field. In the diffused-plasma region, the magnetic field is uniform within a few percent and the plasma is present near the axis of glass tube (50 mm in diameter). At the discharge current of 4.5A, the electron density is equal to about  $10^{13} \text{ cm}^{-3}$ , and the degree of ionization is of the order of ten percent, while the electron temperature of the plasma is about  $1 \times 10^4 \text{ }^\circ\text{K}$ , and does not depend on the electron density. The principle of the apparatus is similar to the TP-D machine<sup>10)</sup> at the Institute of

Plasma Physics, Nagoya University.

An electron beam is produced by the Pierce gun in the beam-produced region, and is injected into the plasma-diffused region through a hole of 2 mm in diameter. This electron gun is set outside the air-coil magnet, so the electron ejected from the gun feels the increasing magnetic field as it runs to the plasma-diffused region. Therefore, a part of the initial energy of the electron is transformed to the energy perpendicular to the magnetic field. When the voltage of the beam  $V_b$ , is changed from 30V to 600V, the current of the beam  $I_b$ , changes from 0.07 mA to 6.0 mA. (The perveance of the gun being about  $4 \times 10^{-7}$ .) The electron density  $n_b$ , of the beam is about  $5 \times 10^8 \text{ cm}^{-3}$  at  $I_b = 2.5 \text{ mA}$ . The gun is operated continuously or pulsively.

Microwave emissions from the beam-plasma system are received by two radiometers which are operated at the two receiving frequencies of  $f = 4.1$  and  $f' = 2f = 8.2 \text{ GHz}$  respectively and have the band widths of 5 MHz. Measurements are made in the following way: The discharge current is kept at the fixed value of  $I_0$  and the magnetic field is swept. The output power of the radiometer is plotted as a function of the magnetic field on the XY-recorder continuously. When the accurate power of the emission intensity is measured, its power is compared with and equalized to that of the noise standard by inserting a known value of attenuation in the transmission line from the plasma to the radiometer. By the simultaneous measurement on the emission at the frequency of 4.1 GHz and 8.2 GHz, we have studied the phenomenon which occurs at the same time for these two frequency bands.



### §3 Experimental results

#### 3.1 Emission from the plasma, the electron beam and the beam-plasma system

Measurements are made on the microwave emission from the plasma in the absence of the electron beam and from the electron beam in the absence of the plasma respectively. In Fig. 2 are shown those spectra as a function of the magnetic field. In the curve (a), which is the emission spectrum for the beam only, the cyclotron emission is seen at  $f_c/f = 1$ , where  $f_c$  is the electron cyclotron frequency. The curve (b) shows the emission spectrum for the plasma without the electron beam. Since the emission near the cyclotron harmonics ( $f_c/f = 1/n$ ) are weak, the plasma electrons are considered to be nearly in thermal equilibrium. On the other hand, the degree of ionization of this plasma becomes to be of the order of ten percent, as described in §2. Therefore, we have obtained the plasma which is Maxwellian and highly ionized.

When the electron beam is injected into this plasma, the emission spectrum changes from the curve (b) <sup>to</sup> the curve (c) which shows that the strongly enhanced emissions are observed near the cyclotron harmonics. It is noted that for measuring the curve (c), the sensitivity of the receiver is lowered by 21 dB as compared with that for the curve (b). Moreover, the time-resolved measurements shows that this enhanced emission is not stationary but pulsating in time, while the injected electron beam is stationary.

#### 3.3 The relation between the enhanced emission and plasma density

In Fig. 3 are shown the emission spectra of the above-mentioned

enhanced emission for the various discharge current. At the rather small discharge current, the enhanced emission (denoted by the peak "2") appears near  $f_c/f = 1$  as shown in curve (a). As the discharge current increases, this peak approaches to the second harmonic  $f_c/f = 1/2$ , as seen in the curves (b) and (c). While, as the discharge current increases, the intensity of the emission also increases until it reaches the maximum value at a certain discharge current. However, when  $I_d$  increases further, its intensity becomes rather weak. At the same time, the emission near the third harmonic begins to be enhanced strongly. Thus, with the increasing discharge current, higher and higher harmonic is enhanced strongly, while the lower harmonic disappears, as shown in the curves (c)  $\sim$  (e).

The above-mentioned characteristics, observed experimentally, of the enhanced emission near the harmonics ( $n = 2, 3, 4, \dots$ ) are seen clearly in Figs. 4 and 5. In Fig. 4, the normalized magnetic field  $f_c/f$ , where the enhanced emissions appear, is plotted as a function of discharge current. In Fig. 5, the intensity of enhanced emissions, normalized to that of the noise standard, are plotted as a function of  $I_d$ .

### 3.3 Relations between the enhanced emission and beam parameters

Next, we investigate the variation of the enhanced emission on the beam parameters, i.e., velocity  $\sqrt{V_b}$ , and density of the electron beam  $n_b$ . For the fixed value of  $V_b$ , the intensity of this emission near the second harmonic is plotted as a function of  $I_b$  as

shown in Fig. 6. Here, in order to vary  $I_b$  while  $V_b$  is kept at a certain value, a perveance of the gun is varied by changing the temperature of the cathode. It is seen from this figure that the enhanced emission becomes to be observed at  $I_b = 0.1$  mA and the intensity of this emission increases exponentially with the beam current  $I_b$ . In the case of  $V_b = 240$  V the intensity of emission becomes to be saturated and amounts to  $P/P_{ns} = 20$  dB as the beam current increases. Such a behavior is also observed in the case of  $V_b = 360$  V and the saturated emission intensity is larger than 30 dB.

In Fig. 7, the intensity of the enhanced emission is plotted as a function of  $V_b$ , keeping the beam density  $n_b$  ( $\propto I_b/\sqrt{V_b}$ ), at the fixed values. The enhanced emission becomes to be observed at  $V_b = 160$  V and its intensity increases exponentially with the beam voltage  $V_b$ . However, its increasing rate with  $V_b$  becomes small above a certain value of  $V_b$ . This values of  $V_b$  are about 240 V for  $n_b = 1.4 \times 10^8 \text{ cm}^{-3}$  and about 280 V for  $n_b = 1.8 \times 10^8 \text{ cm}^{-3}$  respectively.

### 3.4 Doppler shift of cyclotron harmonics waves

It is observed experimentally that when the beam velocity is changed, the magnetic field, where the enhanced harmonic emissions appear, is shifted. The value of this shift from the magnetic field of  $\omega_c/\omega = 1/n$ , increases nearly proportional to  $\sqrt{V_b}$ , therefore this is considered to be the Doppler shift. In Fig. 8, the shift in  $\omega_c/\omega$  is plotted as a function of  $\sqrt{V_b}$ .

### 3.5 Generation of the second harmonics of the strongly enhanced cyclotron harmonic emissions

When the enhanced emission near the second harmonic  $f_c/f=1/2$ , is observed for the receiving frequency  $f = 4.1$  GHz, the emission peak for the receiving frequency  $f' = 8.2$  GHz, which is two times of  $f$ , is observed simultaneously. In Fig. 9, the upper curve shows the emission spectrum of the frequency of  $f' = 2f$  and the lower the spectrum of  $f$ . The emission peak, denoted by "2'", in the spectrum of  $f'$  appears at the magnetic field near  $f_c/f = 1/2$ , where the enhanced emission denoted by "2", is observed in the spectrum of  $f$ . The intensity of the former emission peak "2'" is smaller by 30 dB than that of the latter "2". It must be noted that the peak "2" in the spectrum of  $f'$  is corresponding to the enhanced emission "2" in the curve (a) in Fig. 3. In Fig. 10, the magnetic field, where the enhanced emission is observed as shown in Fig. 9 is plotted as a function of the discharge current  $I_d$  for the cases of  $f = 4.1$  and  $f' = 2f = 8.2$  GHz respectively. It is known that both enhanced emissions "2" for  $f$  and "2'" for  $f'$  occur at the same magnetic field near  $f_c/f = 1/2$ . For these two emissions of  $f$  and  $f'$ , the emission intensities as a function of the discharge current  $I_d$  are shown in Fig. 11, and those as a function of the beam velocity  $\sqrt{V_b}$  are shown in Fig. 12.

Further, these two emissions are represented on a dual beam synchroscope at the same time as shown in Photo 1. The upper trace shows the emission for  $f'$  and the lower that for  $f$ . Both emissions are pulsating in time and occur at the same time.

#### §4 Discussions

When a weak electron beam is injected into a Maxwellian plasma, the strongly enhanced emissions are observed near cyclotron harmonics, as described in the previous section. It is considered that these emissions result from the excitation of the electrostatic waves near cyclotron harmonics due to instability which is expected in beam-plasma systems.

As shown in Fig. 8, for this enhanced emission the Doppler shift is observed, and its frequency shift is described by

$$\omega - 2\omega_c = -k_{||} v_b. \quad (1)$$

It is known from the form of the frequency shift given by Eq. (1), that the instability considered here is not ascribed to the interaction of the cyclotron harmonic waves in a plasma with the slow space charge wave in a beam, but to the interaction of the cyclotron harmonic waves in a plasma with the cyclotron harmonic waves having negative energies in a beam. It has been suggested theoretically by Bers et al.<sup>11)</sup> that such an instability due to the latter interaction can occur for the waves propagating obliquely to the static magnetic field. But the dispersion relation given by them is so complicated that it cannot be applied to the analysis of our experimental results. It may be considered from their theories that the essential character of this instability is obtained for the case where the waves propagate perpendicular to the magnetic field. Therefore, in order to analyze the experimental results, we adopt the model suggested by Crawford et al.,<sup>9)</sup> where the monoenergetic electron beam is injected into a Maxwellian plasma, and there occurs the above-mentioned instability



which results in the excitation of the waves propagating perpendicular to the magnetic field.

The distribution function of electrons in velocity space is assumed to be<sup>9)</sup>

$$f = \alpha \left( \frac{m}{2 K T} \right)^{3/2} \exp \left( - \frac{m(v_{\perp}^2 + v_{\parallel}^2)}{2 K T} \right) + (1-\alpha) \frac{1}{2 v} \delta(v_{\parallel} - v_{0\parallel}) \delta(v_{\perp} - v_{0\perp}), \quad (2)$$

where  $\alpha$  means the ratio of the electron density of the Maxwellian plasma to that of the beam-plasma system. The dispersion relation for the electrostatic waves propagating perpendicular to the magnetic field ( $k_{\parallel} = 0$ ), is given by<sup>3)</sup>

$$1 = \frac{\omega_p^2}{\omega_c^2} \left[ \sum_{n=0}^{\infty} \frac{2\lambda^2 (-1)^n I_n^2(\lambda)}{\lambda^2 [(n\omega_c)^2 - 1]} + (1-\alpha) \sum_{n=1}^{\infty} \frac{\frac{\lambda^2}{2} J_n^2(u)}{\frac{u^2}{2} [(\frac{\omega}{n\omega_c})^2 - 1]} \right], \quad (3)$$

where  $\lambda = (k_{\perp} v_{0\parallel} / \omega_c)^2$ ,  $u = k_{\perp} v_{0\perp} / \omega_c$  and  $\omega_p$  is the electron plasma frequency of a beam-plasma system.

In Fig. 13, the regions of instability, given by Eq. (3) are plotted by the following way: First, the dispersion characteristic for the Maxwellian plasma is calculated by Eq. (3) and plotted on the Allis diagram, where the parameter  $\lambda$  is fixed at  $\lambda = (\rho_c / \lambda \omega)^2 = 0.25$ . Second, using the criterion of the instability given by Crawford et al.,<sup>9)</sup> the region for this instability to occur is

shown by hatching. Under our experimental conditions where the density of the electron beam is very small compared with that of the background plasma and the velocity of the beam is very large compared with the thermal velocity of the plasma, we can assume that  $\alpha \approx 0.9$  and  $v_{0\perp}/v_{th} \approx 25$ . These hatched regions agree qualitatively with those in Fig. 4 where the enhanced emissions are observed.

In Fig. 14, is shown the growth rate of the cyclotron harmonics as functions of the plasma density. Here, the approximate value of growth rate  $\alpha_1$  of the  $n$ th harmonic is calculated from the resonant terms in Eq. (3) by

$$1 = \left(\frac{\omega_p}{\omega_c}\right)^2 \left[ \alpha \left( \frac{2\lambda p(-\lambda) I_n(\lambda)}{\frac{\lambda}{2} \left[ \left(\frac{\omega}{n\omega_c}\right)^2 - 1 \right]} + \frac{\exp(-\lambda) I_{n+1}(\lambda)}{\frac{\lambda}{2} \left[ \left(\frac{\omega}{(n+1)\omega_c}\right)^2 - 1 \right]} \right) \right. \\ \left. + (1-\alpha) \left( \frac{2\lambda J_n(\lambda)}{\frac{\lambda}{2} \left[ \left(\frac{\omega}{n\omega_c}\right)^2 - 1 \right]} + \frac{2\lambda J_{n+1}^2(\lambda)}{\frac{\lambda}{2} \left[ \left(\frac{\omega}{(n+1)\omega_c}\right)^2 - 1 \right]} \right) \right]. \quad (4)$$

Comparing the calculated curves thus obtained in Fig. 14 with the experimental curves in Fig. 5, we can see that the dependence of the growth rate on the plasma density agrees qualitatively with that of the intensity of the harmonic emissions on the discharge current. It was reported by Ikegami<sup>12)</sup> that such a behaviour was observed on the microwave emission from a mercury vapor discharge and was discussed theoretically from the view point of radiation from plasma electrons.

Next, the value of  $k_{\parallel}$  of the cyclotron harmonic wave is calculated to be  $k_{\parallel} = 21.5 \text{ cm}^{-1}$  by using Eq.(1) and the experimental value of the Doppler shift shown in Fig. 8. On the other hand,

it is assumed that  $k_{\perp}$  is estimated from the value at which the instability is expected to occur. Such a value of  $\mu$  is obtained from Eq. (4) to be larger than about 3.0, and  $v_0/v_{th}$  is assumed to be 25. Therefore  $k_{\perp}$  must be larger than  $4 \times 10^3 \text{ cm}^{-1}$ . Since  $k_{\perp}$  is much larger than  $k_{\parallel}$ , it may be considered that the harmonic waves interested here propagate almost perpendicular to the magnetic field and their approximate dispersion relation is given by Eq. (3).

Finally, the second harmonics of the strongly enhanced cyclotron harmonics will be discussed. This emission, which is shown as the peak "2'" in the emission spectrum of  $f' = 2f$  in Fig. 9 is observed when the fundamental emission (the peak "2" in the spectrum of  $f$ ) is enhanced extremely, as shown in Fig. 11. Therefore, it is considered that the generation of the former emission results from a nonlinear effect of the latter emission. It was reported by Terunishi<sup>13)</sup> that such a generation of second harmonic was also observed when the cyclotron harmonic waves are excited strongly by illuminating the plasma with an external microwave. It is considered from our experimental result that the plasma is strongly unstable though the electron beam is very weak compared with the background plasma. On the other hand, the theoretical studies show that the plasma comes to be in a weak turbulent state, as the nonlinear oscillations develop strongly in the plasma. Recently, Apel<sup>14)</sup> has reported that by the convective instability in a beam-plasma system, the wave near the plasma frequency is excited so strongly that its harmonics up to the 8th are observed and this system becomes turbulent. It is also expected in our experiment that the instability near cyclotron harmonic frequencies will

develop and the plasma becomes turbulent as the electron beam becomes much intense. A detailed study of the phenomenon is under way.

The results described in this paper are summarized as follows: The cyclotron harmonic waves are enhanced strongly, when the weak electron beam is injected into the nearly thermalized plasma. It can be interpreted such that these waves are ascribed to an absolute instability due to the interaction between the cyclotron harmonics in the plasma and those in the beam having negative energies. These experimental results are analysed by the model of Crawford et al.<sup>9)</sup> When the cyclotron harmonics are enhanced strongly, their second harmonic emission are observed as a result of a nonlinear effect in plasmas.

### Acknowledgements

The author wish<sup>es</sup> to express his sincere thanks to Prof.

I. Takahashi for his guidance and encouragement, and also to Dr. S. Tanaka for his valuable discussions. The author wishes to thank Prof. K. Mitani and Dr. H. Kubo for their interests and kind discussions. Thanks are also due to the members of our laboratory, especially to Mr. Y. Terumichi for his helpful discussion and to Mr. K. Ohkubo for his help in the experiment. He thanks Dr. S. Ohara, Electrical Communication Laboratory, for his kindness to prepare electron guns.



## References

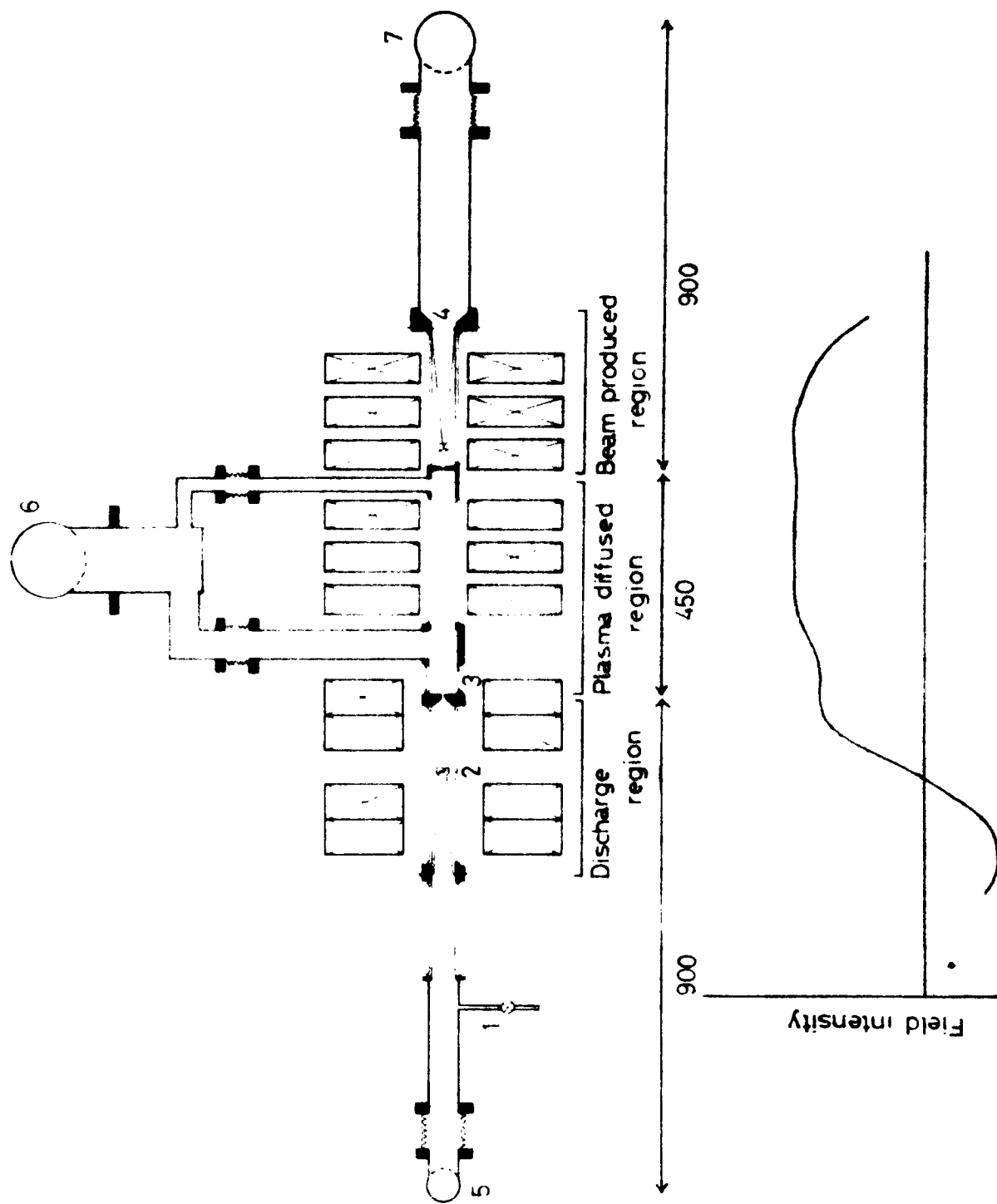
- 1) G. Landauer: J. Nucl. Energy, Pt. C, 4 (1962) 395.
- 2) E. Canobbio, R. Croci: Proc. 6th Intern. Conf. on Ionization Phenomena in Gases, Paris, July 1963.
- 3) K. Mitani, H. Kubo, S. Tanaka: J. Phys. Soc. Japan 19 (1964) 211.
- 4) I. B. Bernstein: Phys. Rev. 109 (1958) 10.
- 5) G. Bekefi, J. D. Coccoli, E. B. Hooper, S. J. Buchsbaum: Phys. Rev. Letters 9 (1962) 6.  
H. Dreicer: Bull. Am. Phys. Soc. 9 (1964) 321.
- 6) S. Gruber, M. D. McBee, L. T. Shepherd: Appl. Phys. Letters 4 (1964) 137.
- 7) G. Bekefi, E. B. Hooper: Appl. Phys. Letters 4 (1964) 135.
- 8) E. G. Harris: Phys. Rev. Letters 2 (1959) 34.
- 9) F. W. Crawford, J. A. Tataronis: Proc. 7th Intern. Conf. on Ionization Phenomena in Gases, Beograd, August 1965.
- 10) M. Ohtuka, K. Takayama et al.: Proc. 7th Intern. Conf. on Ionization Phenomena in Gases, Beograd, August 1965.
- 11) A. Bers, S. Gruber: Appl. Phys. Letters 6 (1965) 27.
- 12) H. Ikegami, F. W. Crawford: Proc. 7th Intern. Conf. on Ionization Phenomena in Gases, Beograd, August 1965.
- 13) Y. Terumichi, T. Ikemura, S. Tanaka, I. Takahashi: J. Phys. Soc. Japan 21 (1966) 2931.
- 14) J. R. Apel: Phys. Rev. Letters 19 (1967) 744.

## List of Figure Captions

- Fig. 1 Experimental apparatus: 1) gas inlet, 2) cathode, 3) anode, 4) electron gun, 5) 2" diffusion pump, 6) 6" diffusion pump, and 7) 4" diffusion pump.
- Fig. 2 Emission spectra from the electron beam, the plasma and the beam-plasma system, as a function of the static magnetic field,  $f_c/f$ . Here,  $V_b=420V$  and  $I_b=3.6$  mA.
- Fig. 3 Emission spectra from a beam-plasma system as a function of the static magnetic field,  $f_c/f$ , with  $I_d$  as a parameter. Here,  $f=3,200$  MHz,  $V_b=420$  V and  $I_b=3.6$  mA.
- Fig. 4 The magnetic field intensity,  $f_c/f$ , where the enhanced emission is observed, is plotted as a function of the discharge current,  $I_d$ . Here,  $f=3,200$  MHz,  $V_b=420$  V and  $I_b=3.6$  mA.
- Fig. 5 Power of enhanced emission  $P_e/P_{ns}$  normalized to that of the noise standard, is plotted as a function of the discharge current  $I_d$ . Here,  $f=3,200$  MHz,  $V_b=420$  V and  $I_b=3.6$  mA.
- Fig. 6 Enhanced emission power  $P_e/P_{ns}$  is plotted as a function of the beam current  $I_b$  with  $V_b$  as a parameter. Here,  $f=3,200$  MHz and  $I_d=0.6$  A.
- Fig. 7 Enhanced emission power  $P_e/P_{ns}$  is plotted as a function of the beam voltage  $V_b$ , with  $n_b$  as a parameter. Here,  $f=3,200$  MHz and  $I_d=0.6$  A.
- Fig. 8 The magnetic field  $f_c/f$ , where the enhanced emission is observed near  $f_c/f=1/2$ , is plotted as a function of the beam velocity  $\sqrt{V_b}$ . Here,  $f=3,200$  MHz and  $I_d=450$  mA.

- Fig. 9 Emission spectra of the beam-plasma system as a function of the static magnetic field. The lower curve shows the spectrum of  $f=4,097$  MHz and the upper curve,  $f'=2f=8,195$  MHz. At the magnetic field where the strongly enhanced emission is seen on the lower curve, the weak emission is also observed on the upper curve. Here,  $V_b=600$  V,  $I_b=5$  mA and  $I_d=150$  mA.
- Fig. 10 The magnetic field,  $f_c / f$ , where the enhanced emission is observed, is plotted as a function of the discharge current  $I_d$ , for the cases of  $f=4,097$  and  $f'=2f=8,195$  MHz, respectively. Here,  $V_b=420$  V and  $I_b=2.2$  mA.
- Fig. 11 Enhanced emission power  $P_e / P_{ns}$  near  $f_c / f = 1/2$ , is plotted as a function of the discharge current  $I_d$ , for the cases of  $f=4,097$  and  $f'=2f=8,195$  MHz respectively. Here,  $V_b=420$  V and  $I_b=2.2$  mA.
- Fig. 12 Enhanced emission power  $P_e / P_{ns}$  near  $f_c / f = 1/2$ , is plotted as a function of the beam velocity  $\sqrt{V_b}$ , for the cases of  $f=4,097$  and  $f'=2f=8,195$  MHz respectively. Here,  $I_d=130$  mA.
- Fig. 13 Dispersion curves. The instability is expected to occur in the regions of shadow. Here,  $\lambda=0.05$ ,  $v_0 / v_{th}=25$  and  $\alpha=0.9$ .
- Fig. 14 The growth rate  $\omega_i / \omega_r$  near the cyclotron harmonics  $\omega \approx n(\omega_c)$ , is plotted as a function of plasma density  $(\omega_p / \omega_r)^2$ . Here,  $\lambda=0.05$ ,  $v_0 / v_{th}=25$  and  $\alpha=0.9$ .

Photo. 1 The enhanced emissions for both cases of  $f=4,100$  MHz and  $f'=2f=8,200$  MHz are observed simultaneously on the synchroscope. The upper and lower traces show the emission powers for  $f'$  and  $f$  respectively. For both traces, the pulsed emissions occur at the same time. Sweep;  $10\mu\text{sec}/\text{div.}$   $f_c/f \approx 1/2.$





F. 2

Ar Discharge Current, 2.2A

$f = 8200 \text{ MHz}$

Emission from the plasma  
with the electron beam

(Attenuated 10 dB)

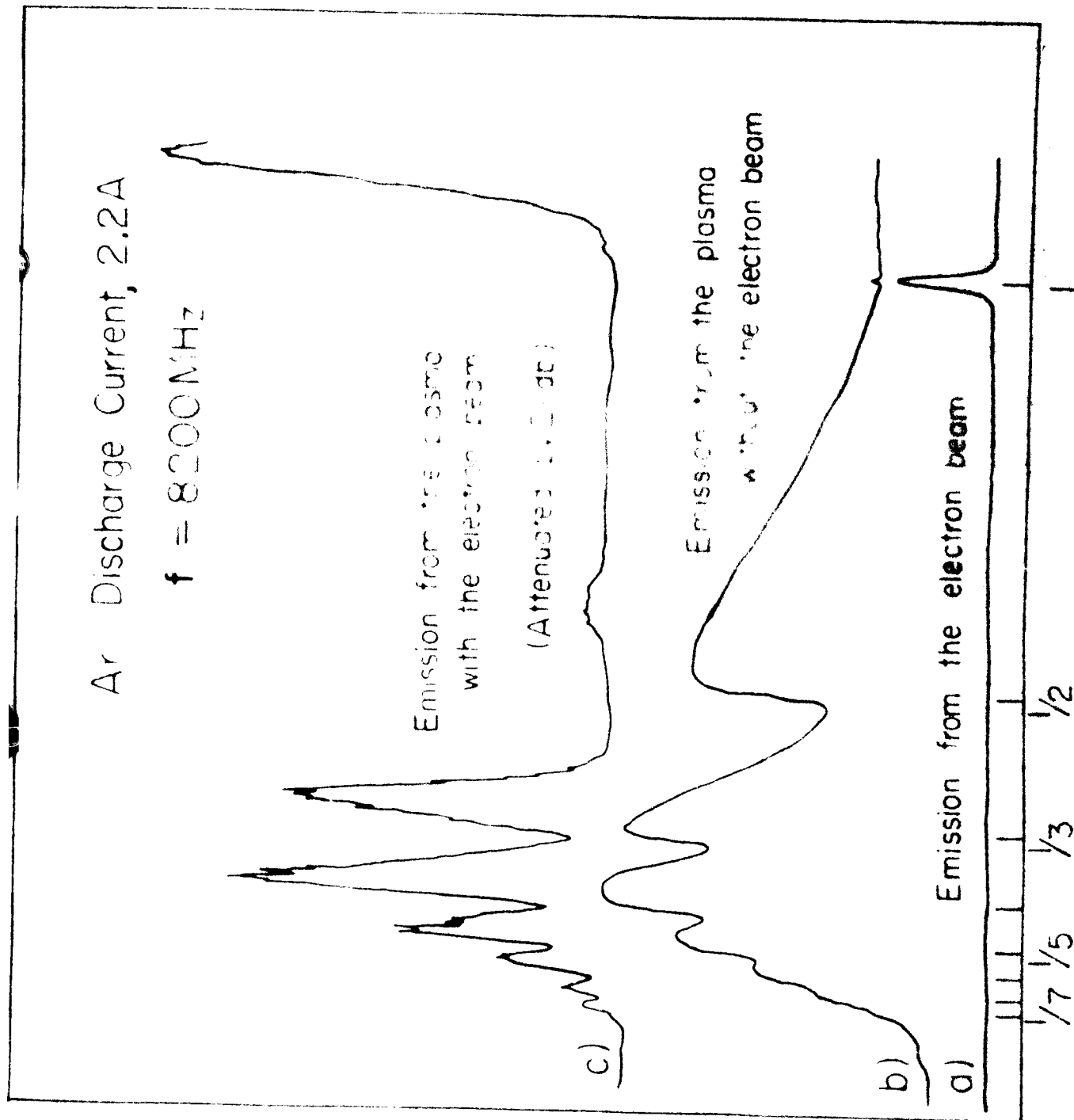
Emission from the plasma

without the electron beam

Emission from the electron beam

Magnetic field  $f_c/f$

Emission power



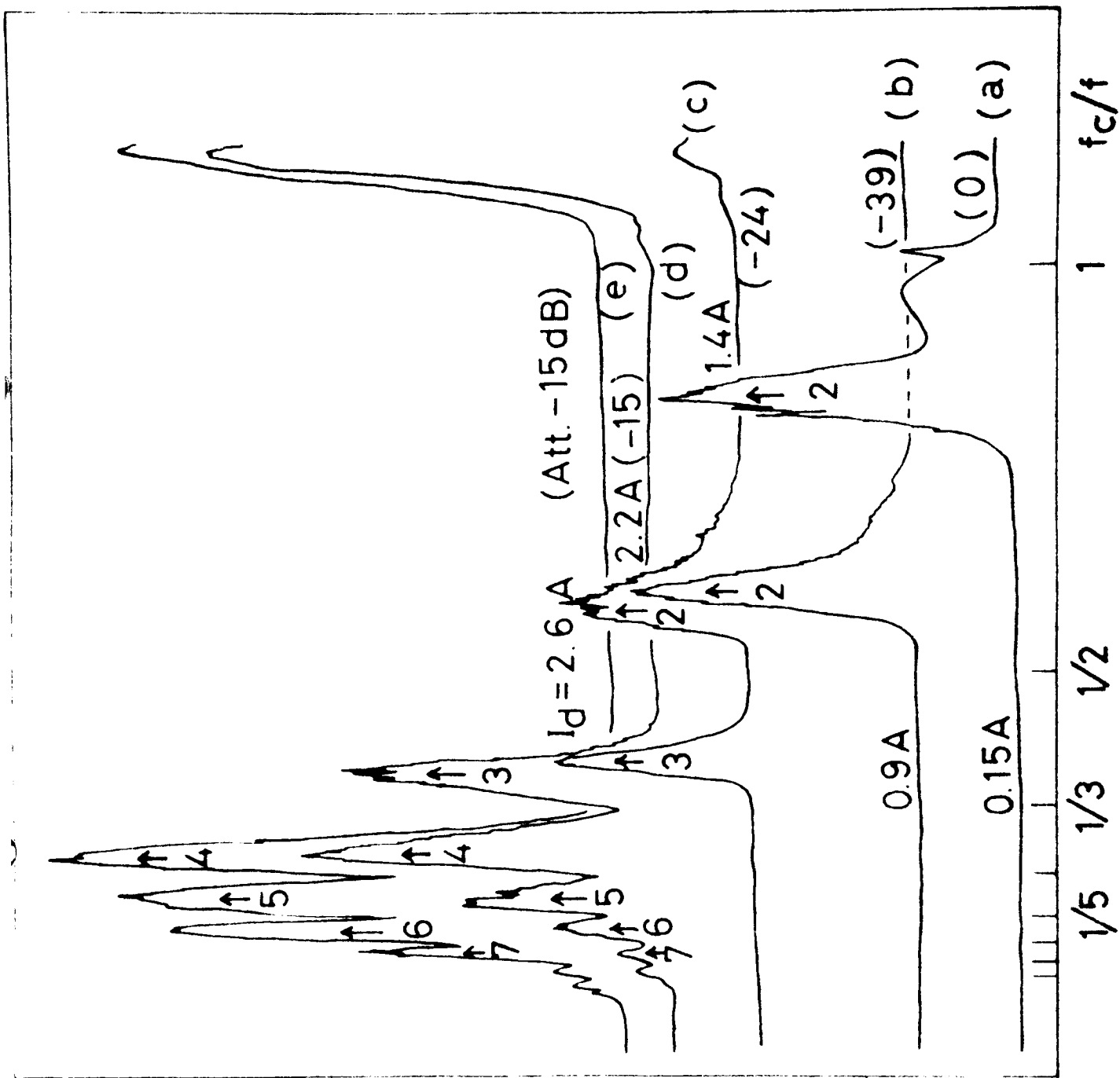
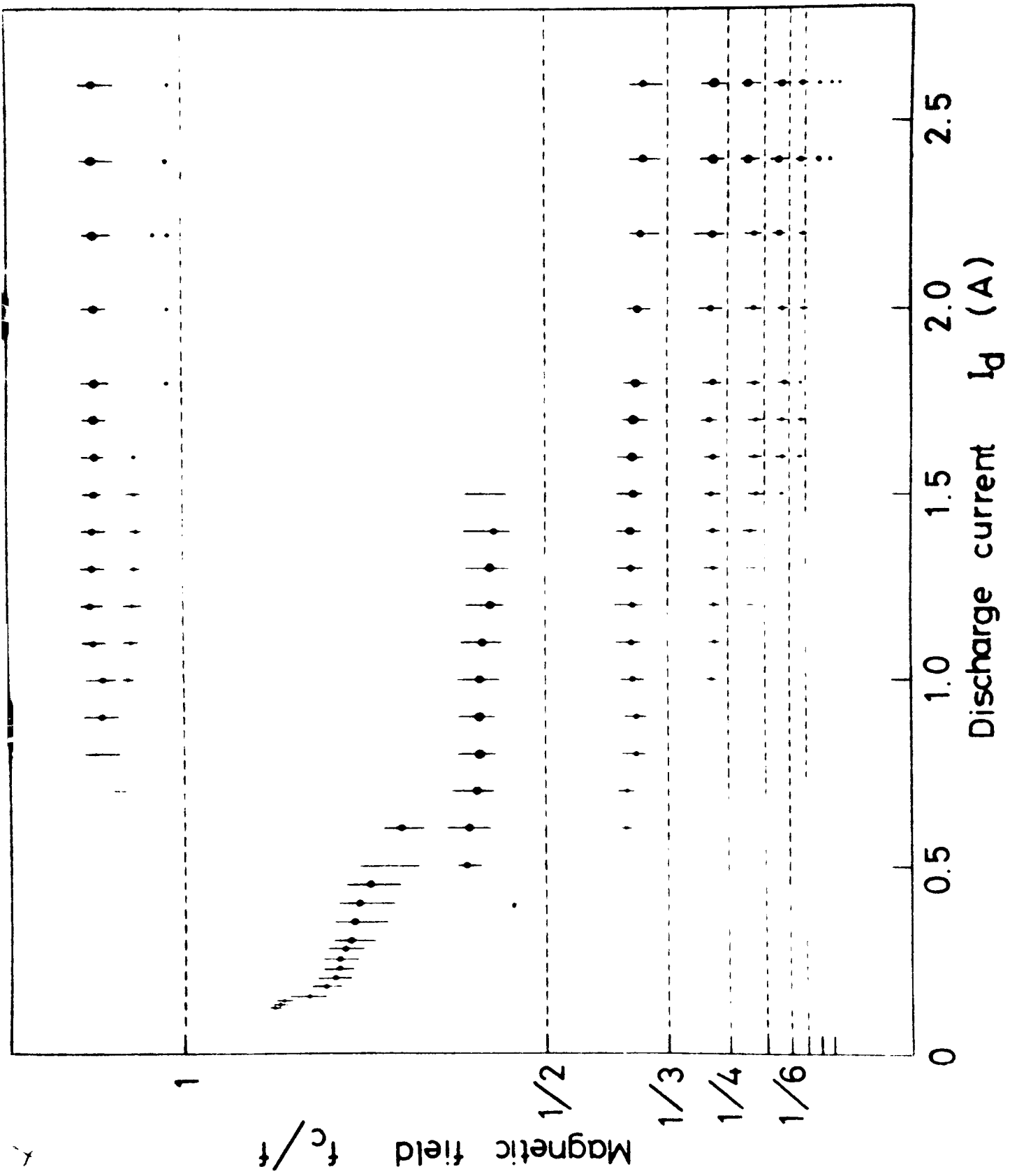


Fig. 2



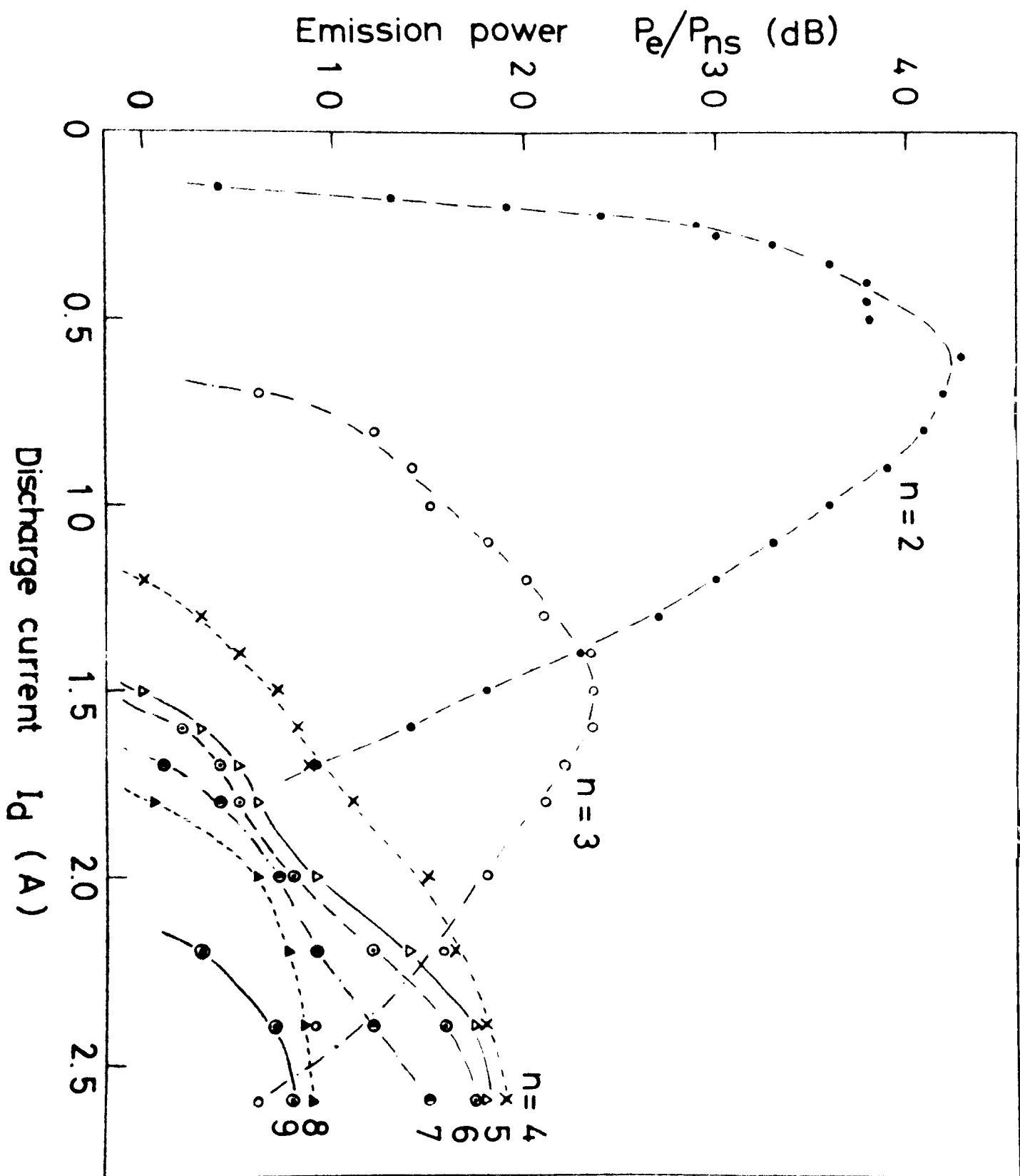


Fig 6

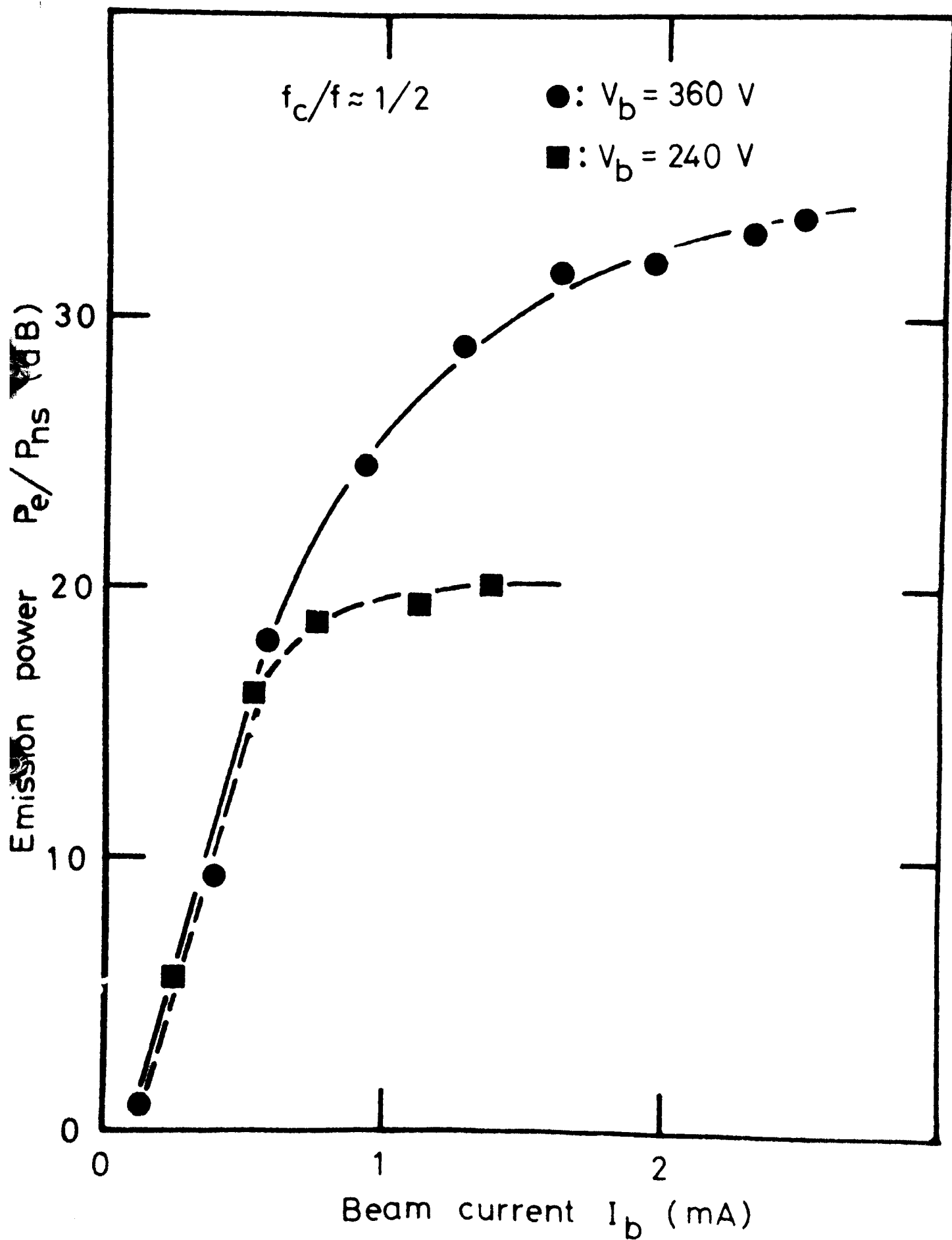
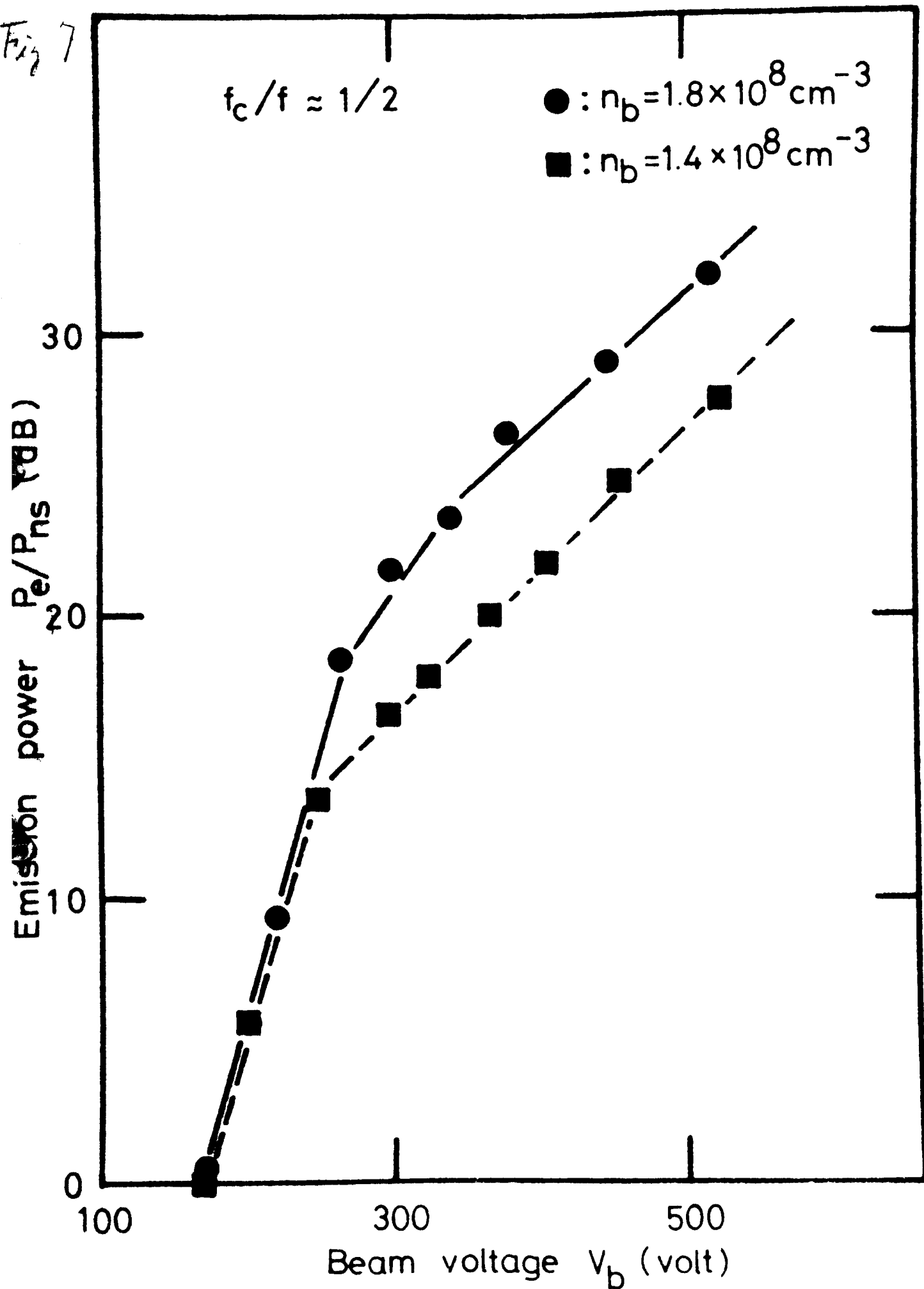




Fig 7



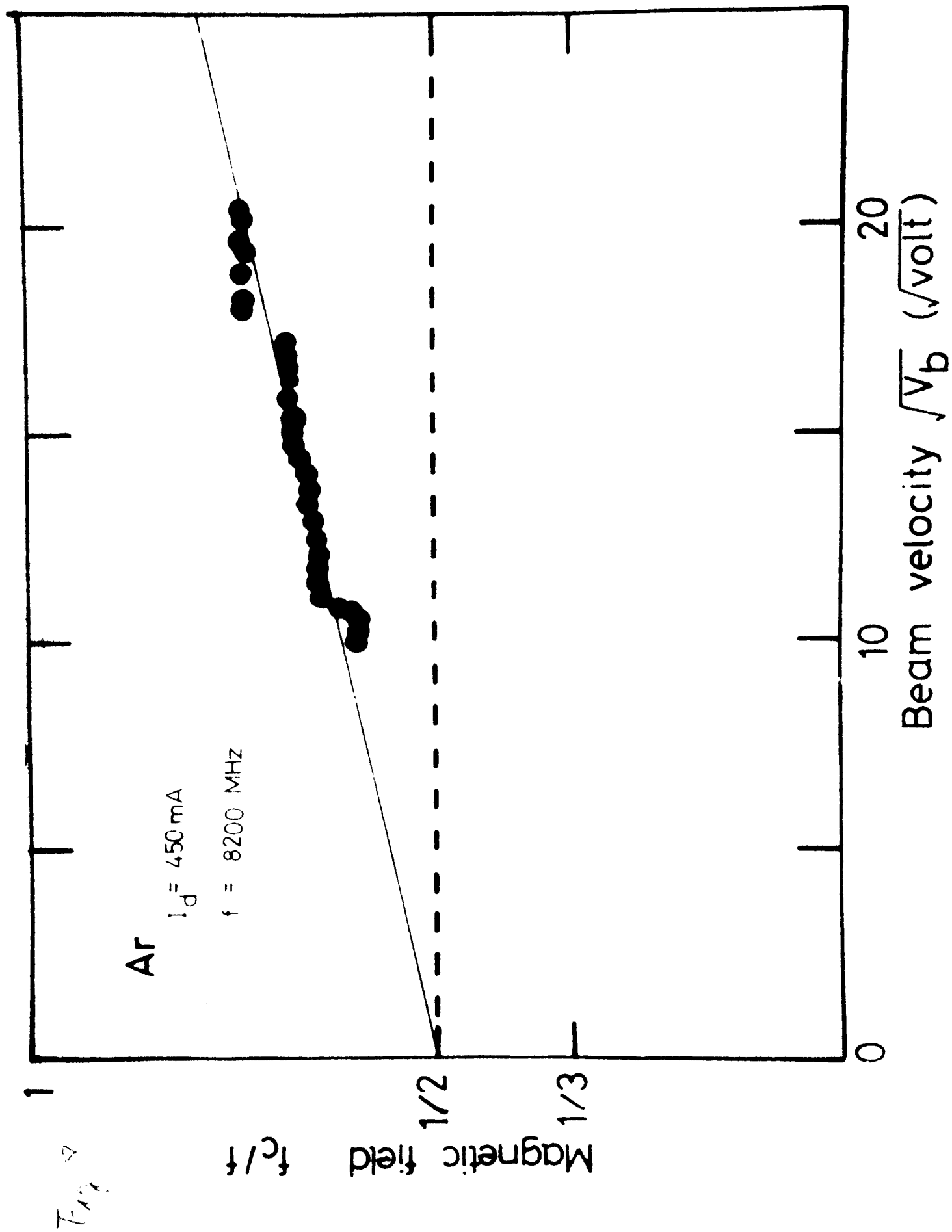
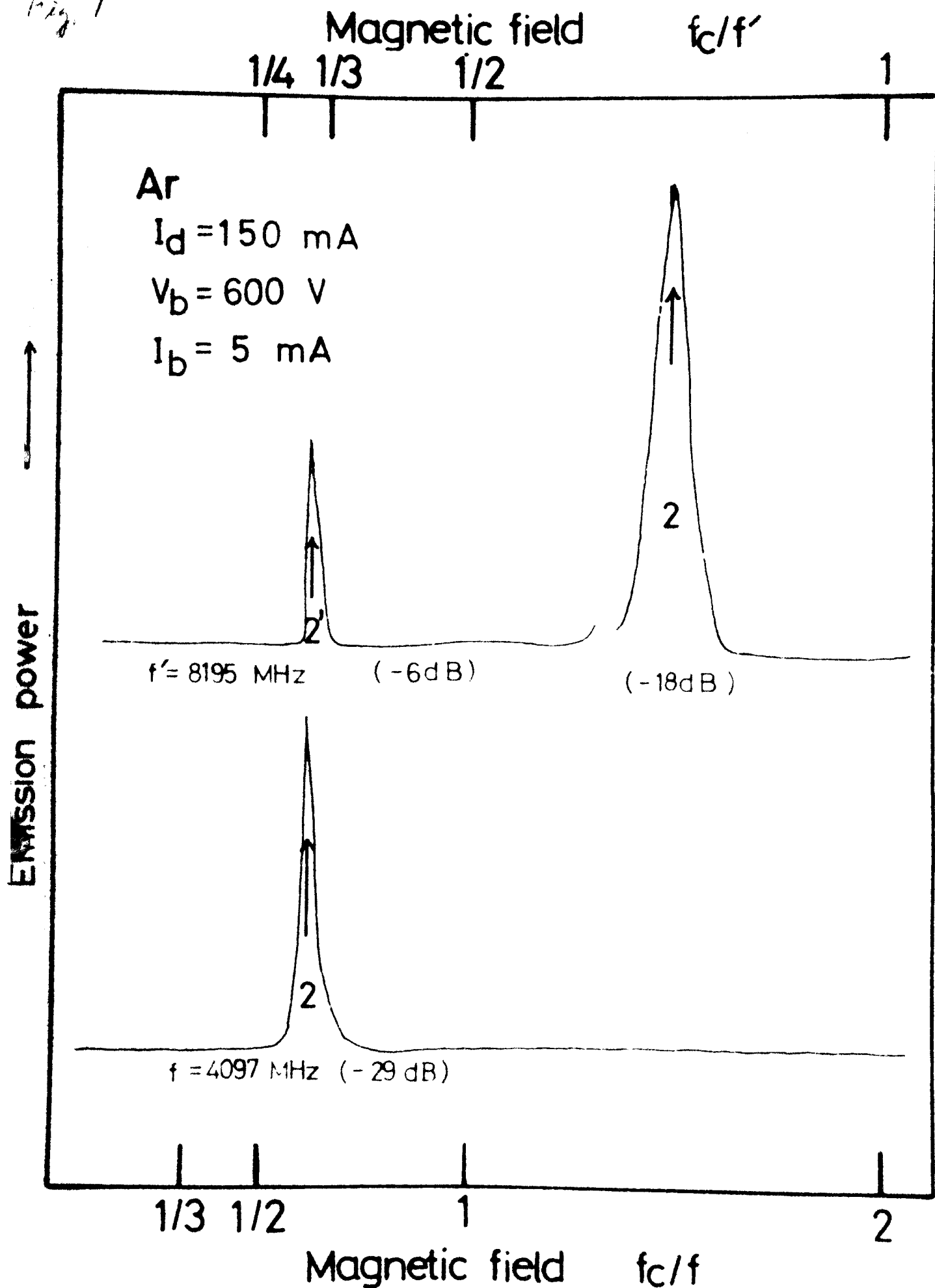
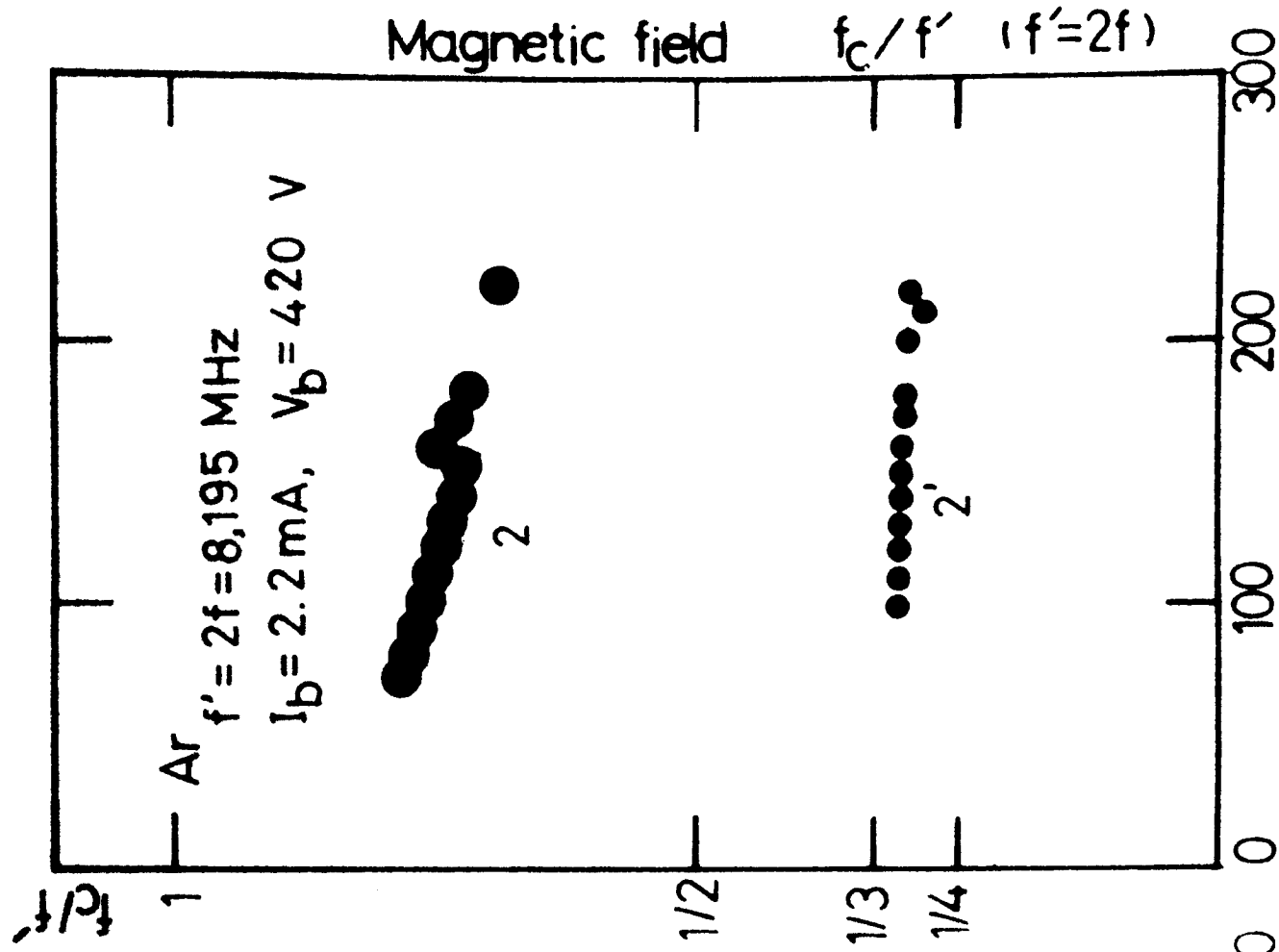
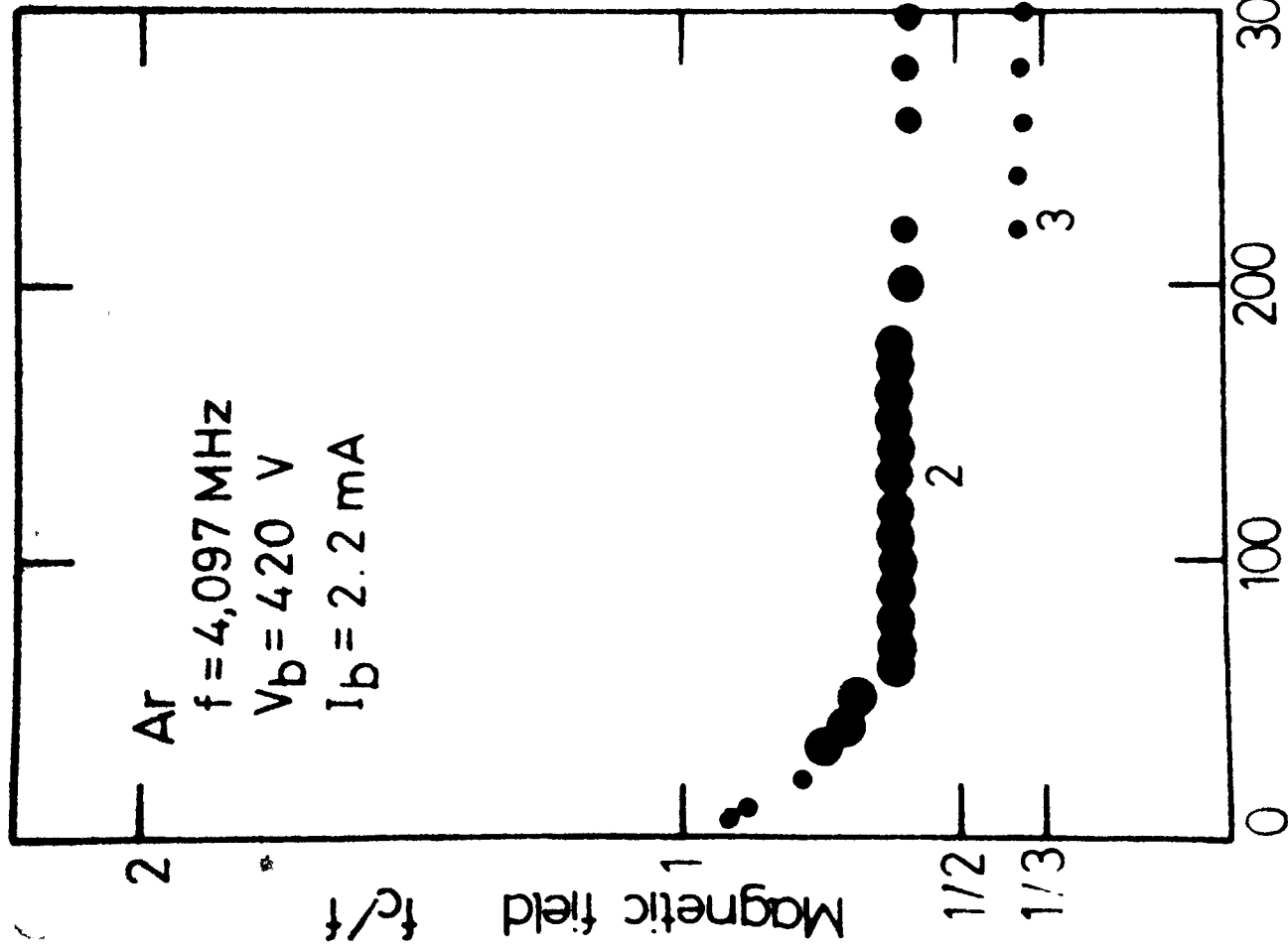


Fig. 9

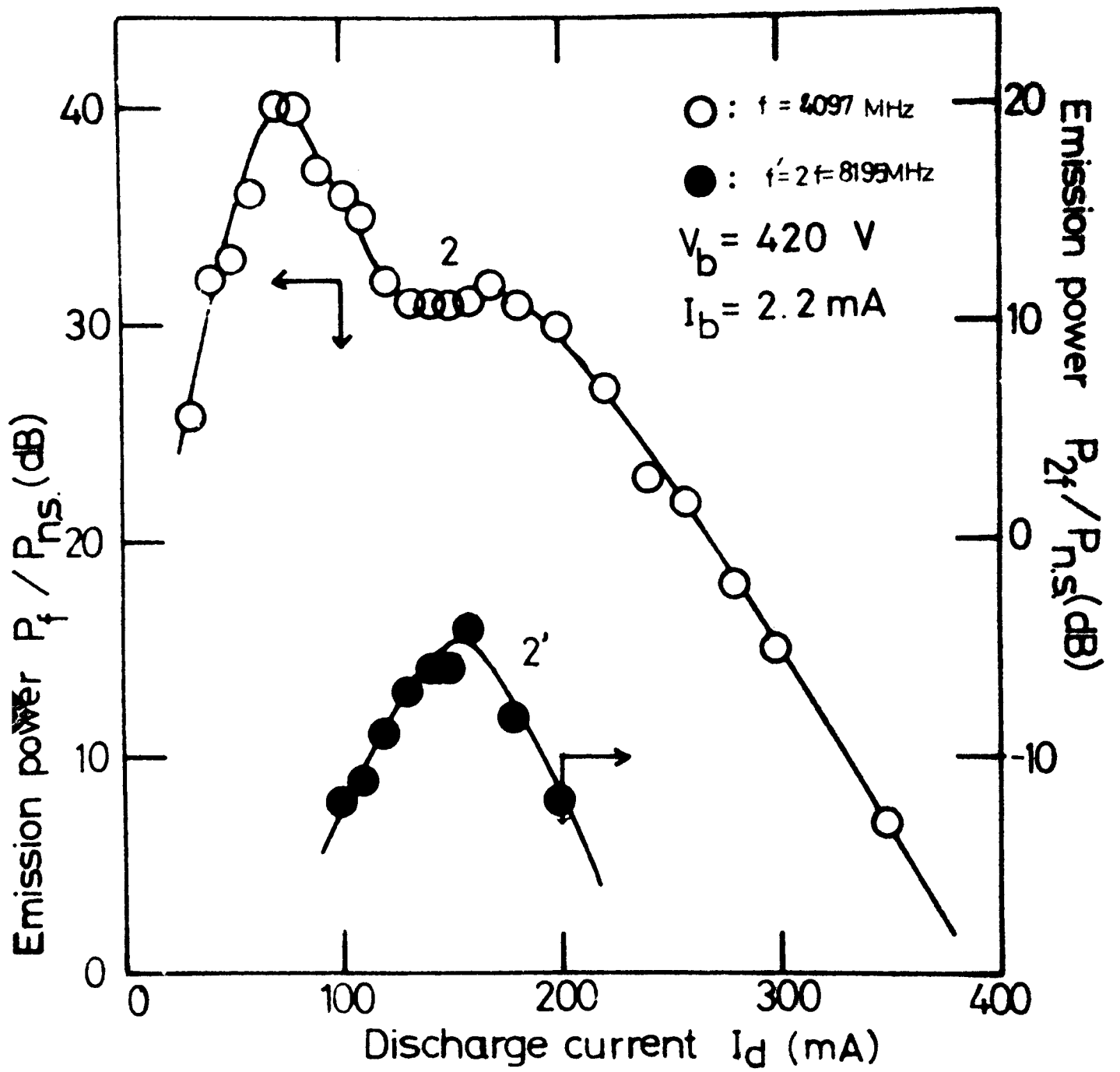


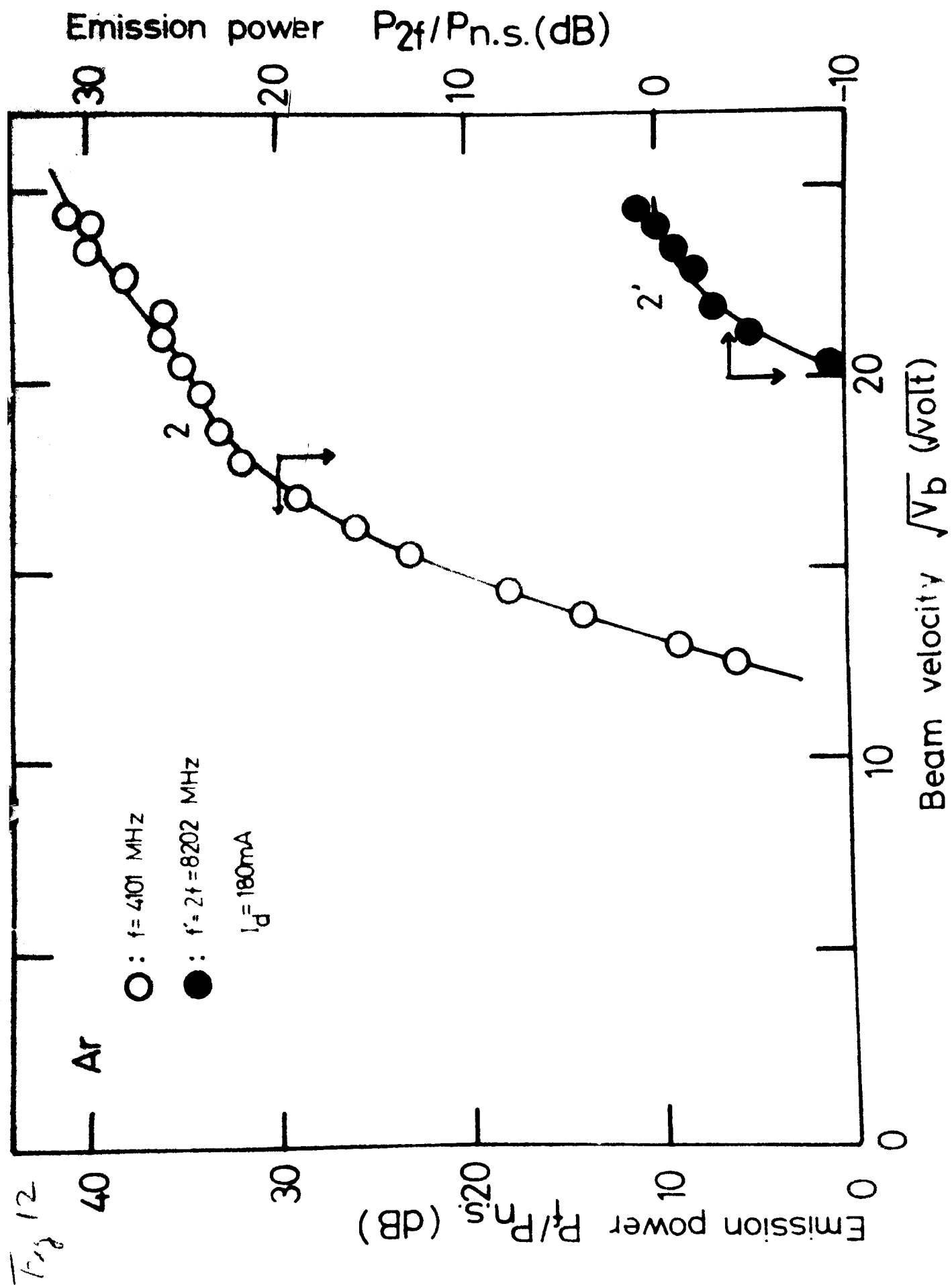
$F_{10}$



Discharge current  $I_d$  (mA)

Fig. 11





Magnetic field  $(f_c/f)^2$

